Nocardamine-Dependent Iron Uptake in Pseudomonas aeruginosa: Exclusive Involvement of the FoxA Outer Membrane Transporter

Vincent Normant, Inokentijs Josts, Lauriane Kuhn, Quentin Perraud, Sarah Fritsch, Philippe Hammann, Gaëtan Mislin, Henning Tidow, Isabelle Schalk

Nocardamine-dependent iron uptake in Pseudomonas aeruginosa: exclusive involvement of the FoxA outer membrane transporter

Journal:	*ACS Chemical Biology*
Manuscript ID	cb-2020-00535j.R1
Manuscript Type:	Article
Date Submitted by the Author:	n/a
Complete List of Authors:	Normant, Vincent; Université de Strasbourg, UMR7242 Josts, Inokentijs; Center for Ultrafast Imaing, , Department of Chemistry, University of Hamburg Kuhn, Lauriane; Universite de Strasbourg, Plateforme Proteomique Strasbourg - Esplanade, Institut de Biologie Moléculaire et Cellulaire Perraud, Quentin; Université de Strasbourg, UMR7242 Fritsch, Sarah; Université de Strasbourg, UMR7242 Hammann, Philippe; Université de Strasbourg, Plateforme Proteomique Strasbourg - Esplanade, Institut de Biologie Moléculaire et Cellulaire Mislin, Gaetan; Université de Strasbourg, UMR7242 Tidow, Henning; University of Hamburg, The Hamburg Centre for Ultrafast Imaging Schalk, Isabelle; Université de Strasbourg, UMR7242

Nocardamine-dependent iron uptake in *Pseudomonas aeruginosa*: exclusive involvement of the FoxA outer membrane transporter

Vincent Normant[1,2], Inokentijs Josts[3,4], Lauriane Kuhn[5], Quentin Perraud[1,2], Sarah Fritsch[1,2], Philippe Hammann[5], Gaëtan L. A. Mislin[1,2], Henning Tidow[3,4], and Isabelle J. Schalk[1,2 *].

[1] CNRS, UMR7242, UMR7242, ESBS, Bld Sébastien Brant, F-67412 Illkirch, Strasbourg, France

[2] Université de Strasbourg, UMR7242, ESBS, Bld Sébastien Brant, F-67412 Illkirch, Strasbourg, France

[3] The Hamburg Centre for Ultrafast Imaging, University of Hamburg, Hamburg, Germany

[4] Department of Chemistry, Institute for Biochemistry and Molecular Biology, University of Hamburg, Hamburg, Germany

[5] Plateforme Proteomique Strasbourg - Esplanade, Institut de Biologie Moléculaire et Cellulaire, CNRS, FR1589, 15 rue Descartes, F-67084 Strasbourg Cedex, France

[*] To whom correspondence should be addressed: isabelle.schalk@unistra.fr.

ABSTRACT

Iron is a key nutrient for almost all living organisms. Paradoxically, it is poorly soluble and consequently poorly bioavailable. Bacteria have thus developed multiple strategies to access this metal. One of the most common consists of the use of siderophores, small compounds that chelate ferric iron with very high affinity. Many bacteria are able to produce their own siderophores or use those produced by other microorganisms (exosiderophores) in a piracy strategy. *Pseudomonas aeruginosa* produces two siderophores, pyoverdine and pyochelin, and is also able to use a large panel of exosiderophores. We investigated the ability of *P. aeruginosa* to use nocardamine (NOCA) and ferrioxamine B (DFOB) as exosiderophores under iron-limited planktonic growth conditions. Proteomic and RT-qPCR approaches showed induction of the transcription and expression of the outer membrane transporter FoxA in the presence of NOCA or DFO in the bacterial environment. Expression of the proteins of the heme- or pyoverdine- and pyochelin-dependent iron uptake pathways was not affected by the presence of these two tris-hydroxamate siderophores. ^{55}Fe uptake assays using *foxA* mutants showed ferri-NOCA to be exclusively transported by FoxA, whereas ferri-DFOB was transported by FoxA and at least one other unidentified transporter. The crystal structure of FoxA complexed with NOCA-Fe revealed very similar siderophore binding sites between NOCA-Fe and DFOB-Fe. We discuss iron uptake by hydroxamate exosiderophores in *P. aeruginosa* cells in the light of these results.

INTRODUCTION

Iron is an essential nutrient for most bacteria. It is used as an enzymatic cofactor and is required for many essential processes; such as deoxynucleotide biosynthesis, DNA replication, and respiration.[1] Iron can exist in two different oxidation states in biological systems, the ferric (Fe^{3+}) or ferrous (Fe^{2+}) forms, both playing an essential role in biological oxidation-reduction processes. Under aerobic conditions, iron is mostly found in its ferric form, which is poorly soluble and consequently insufficiently bioavailable for microorganisms. Under conditions of infection, this metal is sequestered by host proteins, such as transferrin or lactoferrin, due to the insolubility of ferric iron and toxicity of ferrous iron (Fenton reaction). Thus, bacteria mostly grow under iron-restricted conditions, regardless of their biological environment. To overcome the paucity of available iron and improve its bioavailability, bacteria produce molecules called siderophores,[2] characterized by a very high affinity for Fe^{3+} (10^{42} M^{-1} and 10^{32} M^{-1} for enterobactin and pyoverdine, respectively[3,4]). Four main types of siderophores are produced by microorganisms, depending on the chemical groups involved in Fe^{3+} hexa-coordination: (i) catecholate (only catecholate groups are involved in iron chelation), (ii) hydroxamates, (iii) carboxylates, and (iv) mixed siderophores, with various chemical groups involved in iron chelation.[2] Siderophores are synthesized by bacteria and released into their environment to scavenge Fe^{3+}. Because of their very high affinity for iron, siderophores are able to remove iron from minerals in the rhizosphere or from host proteins, such as lactoferrin or transferrin, during infections.

In Gram-negative bacteria, upon the capture of iron from the bacterial environment by siderophores, the ferri-siderophore complexes are recognized and transported back into the bacteria by specific outer membrane transporters.[5] These transporters interact with an inner membrane protein complex of three proteins, TonB, ExbB, and ExbD, providing the energy for ferri-siderophore uptake across the outer membrane.[6,7] These outer membrane transporters are

thus called TonB-dependent transporters (TBDTs). TBDTs generally contain highly specific siderophore binding sites and thus a given TBDT is able to transport only one siderophore or structurally-related siderophores.[5] Most bacteria can also use exosiderophores (siderophores produced by other microorganisms) to access iron in a siderophore piracy strategy.[8,9] A prerequisite of such a strategy is that the genome of the pirate bacteria contains genes encoding TBDTs that are able to recognize and transport the exosiderophores produced by the hacked bacteria. In addition, it is necessary for the pirate bacteria to phenotypically adapt their expression of the corresponding TBDTs and other accessory proteins to gain access to iron from the exosiderophores produced by the hacked microorganism.[9]

The opportunistic human pathogen *Pseudomonas aeruginosa* produces two siderophores: pyoverdine (PVD), considered as a major siderophore, and pyochelin (PCH), considered as a secondary siderophore.[10] The production of these siderophores occurs in parallel with the expression of the specific TBDTs FpvA and FpvB for PVD[11,12] and FptA for PCH.[13] The genome of *P. aeruginosa* also contains three genes encoding TBDTs involved in heme uptake pathways (*hasR*, *phuR* and *hur* -previously called *hxuA*-)[14–16] and various genes encoding TBDTs involved in ferric-iron acquisition by exosiderophores. *P. aeruginosa* can acquire iron from the catechol exosiderophore enterobactin via the TBDTs PfeA and PirA ,[17–20] and vibriobactin via FvbA.[21] It can also use the exosiderophores mycobactin and carboximycobactin via the TBDT FemA,[22] aerobactin, rhizobactin, and schizokinen by ChtA,[23] and citrate by FecA.[24] Hydroxamate siderophores are also used by *P. aeruginosa*, along with ferrioxamine B (DFOB), transported by FoxA,[25,26] and ferrichrome (FRC), transported by FiuA.[25] DFOB (Figure 1B) is produced by the soil bacterium *Streptomyces pilosus*[27] and FRC (Figure 1C) by various fungi, such as *Ustilago*, *Aspergillus*, and *Penicillium*.[28]

Bacteria are able to sense the presence of such exosiderophores by either sigma or anti-sigma factors, two-component systems, or transcriptional regulators of the AraC family.[22,29–31] Having

detected the presence of ferri-exosiderophores, these transcriptional regulators activate the transcription of the corresponding TBDT for iron acquisition.[9,22,29–32]

Here, we investigated the ability of *P. aeruginosa* to use nocardamine (NOCA, Figure 1A) as an exosiderophore. NOCA, also called desferrioxamine E, is a cyclic tris-hydroxamate siderophore related to DFOB, with a higher affinity for iron: 10^{32} M^{-1} for NOCA and 10^{30} M^{-1} for DFOB[33] (Figure 1). NOCA is synthesized by various actinomycetes, such as *Streptomyces*, *Nocardia*, and *Micromonospora*,[34] and bacteria, such as *Streptomyces griseus*,[35] *Pseudomonas stutzeri*,[36] and *Enterobacter agglomerans*.[37] We show that the presence of NOCA in the *P. aeruginosa* environment strongly induces the transcription and expression of *foxA* with the same efficiency as DFOB. We demonstrate, using ^{55}Fe, that NOCA-^{55}Fe is exclusively transported by the TBDT FoxA, whereas DFOB uses, in addition to FoxA, at least one other transporter. We also determined the crystal structure of FoxA complexed with ferri-NOCA, revealing a siderophore-binding site very similar to that of DFOB.

RESULTS AND DISCUSSION

The presence of NOCA induces the transcription and expression of the TBDT *foxA* in *P. aeruginosa* cells. *P. aeruginosa* can sense the presence of iron-loaded exosiderophores in its environment via AraC regulators, sigma factors, or two-component systems, resulting in the induction of the transcription and expression of the corresponding TBDTs.[9,22,29–32] We grew *P. aeruginosa* PAO1 in iron-restricted medium (CAA medium), with or without 10 μM NOCA, and analyzed the bacteria by proteomics to identify the TBDTs and any other proteins involved in iron acquisition by NOCA (Figure 2).

In the presence of NOCA, only the expression of the TBDT FoxA was strongly induced, showing a log2 6.37-fold increase (Figure 2A). This result was confirmed by RT-qPCR, which showed a log2 4.46-fold induction of transcription of *foxA* gene in the presence of NOCA (Figure 3). We repeated the same proteomic and qRT-PCR experiments with DFOB, and observed similar induction of *foxA* transcription and expression (Figures 2 and 3), as previously shown.[22] The induction of transcription and expression of *foxA* was of the same intensity for both exosiderophores.

In conclusion, *foxA* transcription and expression is induced by both NOCA and DFOB, showing that these two siderophores use this TBDT to transport iron from the environment into the *P. aeruginosa* periplasm. Previous studies, using exactly the same experimental approach and conditions, showed that the presence of the tris-hydroxamate exosiderophore FRC in the *P. aeruginosa* environment induces the expression of the TBDT FiuA.[9] These sensing mechanisms involve cell surface signaling that involves the TBDT itself and coupled sigma and anti-sigma factors FoxR/FoxI and FiuR/FiuI.[22,25] The various changes in protein conformation and the protein interactions involved in these signaling cascades have been described in more detail for the PVD pathway, with the FpvR/PvdS or FpvR/FpvI sigma/anti sigma factors. Binding of iron-loaded PVD to the TBDT FpvA induces movement of the periplasmic N-

terminal domain of FpvA interacting with the periplasmic part of the anti-sigma factor FpvR. This interaction results in FpvR proteolysis by two enzymes and release of the two sigma factors PvdS and FpvI, which are normally sequestered by FpvR, into the cytoplasm. PvdS and FpvI then initiate transcription of the *fpvA* gene and all genes encoding proteins involved in iron acquisition by PVD.[12,31,41–47] Certainly, a very similar mechanism is involved in the regulation of the transcription of *fiuA* by ferri-FRC and *foxA* by NOCA and DFOB.

Tris-hydroxamate siderophores do not strongly repress the expression or transcription of proteins involved in the PVD and PCH pathways. Previous studies have shown that the presence of catechol siderophores, such as enterobactin and vibriobactin, significantly represses the expression of the proteins of the PCH pathway and, to a lower extent, those of the PVD pathway.[9] The expression of the proteins of the PCH and PVD pathways was not significantly repressed by the presence of NOCA or DFOB (Figures 2D and 2E). This result was confirmed by RT-qPCR by following the transcription of the mRNAs encoding *fptA* and *fpvA* (the TBDTs of PCH and PVD, respectively) in the presence of NOCA (Figure 3A) or DFOB (Figure 3B). There was also no effect on the expression of the mRNA or proteins of heme-uptake pathways (*hasR* and *phuR* TBDTs, proteomic data and Figure 3). A very similar phenotypic adaptation was previously described for *P. aeruginosa* cells grown in the presence of FRC,[9] leading to the conclusion that hydroxamate siderophores, such as NOCA, DFOB, and FRC do not repress the expression of the proteins of the PCH- and PVD-dependent iron uptake pathways. Non-repression of the expression of the PVD and PCH pathways has also been observed in the presence of yersiniabactin (a mixed siderophore produced by *Yersinia pestis*).[9] These results were previously explained by the different affinities of the siderophores for ferric iron and consequently their ability to scavenge iron from the environment. The catechol siderophores, like enterobactin, show the highest affinity for ferric iron among siderophores,[3] with a K_a of

10^{42} M^{-1} for enterobactin, much higher than the affinities of PVD and PCH, the siderophores produced by *P. aeruginosa* (10^{18} M^{-2} for PCH [48] and 10^{32} M^{-1} for PVD [49]). Consequently, more ferric iron-loaded catechol siderophores are formed in the bacterial environment than ferri-PCH and ferri-PVD. This results in lower expression of the PVD and PCH uptake pathways because of lower activation of the transcriptional regulators AraC for the PCH pathway and the anti-sigma/sigma system for PVD.[30,31] Tris-hydroxamate siderophores compete less for iron chelation than catecholate siderophores or PVD, which explains the absence of repression in the expression of proteins of the PVD pathway and even the PCH pathway when bacteria are grown in the presence of such exosiderophores.

Ferri-NOCA is transported only by the TBDT FoxA in *P. aeruginosa.* *foxA* was the only TBDT for which the transcription and expression was induced by the presence of NOCA. We thus next investigated the effect of *foxA* deletion on ^{55}Fe acquisition in *P. aeruginosa* cells in the presence of NOCA. We used a strain of *P. aeruginosa* unable to produce the siderophores PVD and PCH (*ΔpvdFΔpchA* in Supplementary Table 1) to avoid any ^{55}Fe uptake by these two siderophores. The bacteria were grown in CAA medium and then incubated in the presence of NOCA-^{55}Fe. Aliquots were removed at various timepoints, the bacteria pelleted, and the radioactivity in the bacteria counted. The *ΔpvdFΔpchA* strain was able to acquire ^{55}Fe via NOCA, with an uptake rate of 335.96 ± 59.12 pmol/ml/$OD_{600\ nm}$ (Figure 4A). The deletion of *foxA* (*ΔpvdFΔpchAΔfoxA* mutant) completely abolished the ability of the bacteria to assimilate ^{55}Fe in the presence of NOCA, similarly to carbonyl cyanide-*m*-chlorophenylhydrazone (CCCP) treatment of the bacteria. CCCP is an inhibitor of the inner membrane proton motive force. It is well known that the incubation of bacteria with CCCP abolishes all TonB-dependent transport.[50] Overall, these results demonstrate that ^{55}Fe is transported in *P. aeruginosa* cells in

the presence of NOCA and that such transport is exclusively dependent on FoxA for iron uptake across the outer membrane.

We also demonstrated the exclusive involvement of FoxA in ferri-NOCA uptake using a growth assay. The PVD- and PCH-deficient strain (*ΔpvdFΔpchA*) and its corresponding *foxA* mutant (*ΔpvdFΔpchAΔfoxA*) were grown in CAA medium, which contains approximately 20 nM iron according to ICP-AES measurements.[51] Growth was carried out in the presence or absence of 10 μM NOCA (Figure 5A and 5B), which would chelate all the iron of the medium. *ΔpvdFΔpchA* cells grew in the presence of NOCA, showing that they could access iron via NOCA. On the contrary, the *foxA* deletion mutant *ΔpvdFΔpchAΔfoxA* was unable to grow in the presence of NOCA, confirming that FoxA is the only TBDT present in the *P. aeruginosa* genome that is able to transport ferri-NOCA complexes.

Ferri-DFOB uptake in *P. aeruginosa* involves FoxA and at least one other unidentified TBDT. DFOB induced *foxA* transcription and expression when *P. aeruginosa* cells were grown under iron-restricted conditions in the presence of this exosiderophore (Figures 2 and 3). We used the same ^{55}Fe uptake assay as above to investigate iron acquisition via DFOB in *P. aeruginosa ΔpvdFΔpchA* cells (Figure 4B). Uptake of 220.83 ± 47.04 pmol/ml/OD_{600nm} of ^{55}Fe was observed in the presence of DFOB. This uptake is abolished in the presence of CCCP indicating that it is dependent on the proton motive force of the inner membrane and completely relies on TBDTs. Deletion of *foxA* induced a 27% decrease in ^{55}Fe uptake by *ΔpvdFΔpchAΔfoxA* cells (161.56 ± 56.93 pmol/ml/OD_{600nm}) relative that by *ΔpvdFΔpchA* cells. Such partial inhibition of ^{55}Fe uptake indicates that FoxA is also involved in iron uptake by DFOB, but that it is not the only TBDT involved. Deletion of *fiuA* (*ΔpvdFΔpchAΔfiuA* strain*)* did not affect ^{55}Fe transport by DFOB (213.96 ± 10.88 pmol/ml/OD_{600nm} ^{55}Fe transport after 180 minutes), indicating that this transporter plays no role in iron acquisition by DFOB in *P.*

aeruginosa cells. Growth of *ΔpvdFΔpchA* and *ΔpvdFΔpchAΔfoxA* cells in CAA medium in the presence of 10 μM DFOB (Figure 5C) resulted in slightly less (9%) growth of the *foxA* mutant than *ΔpvdFΔpchA* cells, confirming that FoxA is not the only TBDT involved in iron assimilation by this exosiderophore. At least one other TBDT is involved and takes over uptake in the absence of FoxA expression.

Since this TBDT may have its expression induced only when FoxA is absent and in a strain unable to produce pyoverdine and pyochelin, *P. aeruginosa* Δ*pvdF*Δ*pchA*Δ*fiuA*Δ*foxA* cells were grown in iron-restricted medium (CAA medium), with or without 10 μM DFOB, and analyzed by proteomics (Supplementary Figure 2). The data show that no other TBDT has its expression induced in a *fiuA* and *foxA* mutant, suggesting that the second TBDT involved in iron acquisition by DFOB has not its transcription and expression regulated by the presence of DFOB in the growth media. We also compared the expression of the different TBDTs in the Δ*pvdF*Δ*pchA*Δ*fiuA*Δ*foxA* versus PAO1 in the absence of any siderophore in the growth media, and no TBDT having its expression induced was detected (Supplementary Figure 3). *P. aeruginosa* has in its genome 35 genes coding for TBDTs.[52] Among them, 17 have their transcription negatively regulated by Fur and positively by the presence in the growth media of the siderophore transported *via* either sigma and anti-sigma factors, AraC regulators or two-component systems.[52] 18 genes coding for TBDTs have their transcription only regulated by Fur with no positive auto-regulating loop and for 12 of them the siderophore or molecule transported has not been identified yet. These 12 TBDTs are all possible candidates for the import of iron loaded DFOB.

Overall, these data show that iron assimilation via DFOB does not involve the TBDT FiuA, but FoxA and at least one other unidentified TBDT, of which the expression is not regulated by the presence of this exosiderophore (not detected by the proteomic approach described above).

FoxA is not involved in ^{55}Fe uptake via FRC in *P. aeruginosa.* Previous studies, carried out under the same conditions as described here, have shown that FRC induces *fiuA* expression when *P. aeruginosa* cells are grown under iron-restricted conditions in the presence of this exosiderophore [9]. As above, we followed ^{55}Fe uptake to investigate iron acquisition via FRC in *P. aeruginosa ΔpvdFΔpchA* cells (Figure 4C). Uptake of 110.81 ± 16.77 pmol/ml/OD_{600nm} of ^{55}Fe occurred in the presence of FRC, indicating that FRC is three times less efficient than NOCA and two times less efficient than DFOB in transporting iron in *P. aeruginosa* cells. This uptake is also abolished in the presence of CCCP indicating that it relies on TBDTs.[50] Mutation of *fiuA* resulted in a 20% decrease in ^{55}Fe acquisition by FRC (88.07 ± 5.89 pmol/ml/OD_{600nm}) after 180 min of uptake, proving that FiuA can transport FRC-Fe^{55} complexes into the pathogen. In contrast, there was no significant difference in FRC-^{55}Fe acquisition between *ΔpvdFΔpchA* and *ΔpvdFΔpchAΔfoxA* and between *ΔpvdFΔpchAΔfiuA* and *ΔpvdFΔpchAΔfiuAΔfoxA* cells (Figure 4C), indicating that FoxA is apparently not involved in iron acquisition by FRC. The growth of *ΔpvdFΔpchA* and *ΔpvdFΔpchAΔfiuA* cells in CAA medium in the presence of 10 µM FRC showed a low level (14%) of growth inhibition (Figure 5D and 5E), confirming that FiuA is not the only TBDT involved in iron assimilation by FRC. In order to identify this transporter, *P. aeruginosa* cells deleted for both *foxA* and *fiuA* (Δ*pvdF*Δ*pchA*Δ*fiuA*Δ*foxA*) were grown in iron-restricted medium (CAA medium), with or without 10 µM FRC, and analyzed by proteomics (Supplementary Figure 2). The data show, as above for DFOB, that no other TBDT has its expression induced in a *fiuA* and *foxA* mutant in the presence of FCR.

In conclusion, FoxA plays no role in iron uptake via FRC, but FiuA is involved, and at least one other TBDT, of which the transcription and expression is not induced by the presence of FRC in the growth media.

Structure of FoxA complexed with NOCA. DFOB and NOCA are structurally related siderophores. We investigated the interactions between FoxA and NOCA by determining the crystal structure of the complex to 2.95 Å resolution (Figure 6). The electron density for the siderophore was present, as shown by Polder omit maps, revealing a cloverleaf-like shape of the cyclic NOCA within the binding pocket of FoxA (Figure 6). Our crystal structure of the FoxA-NOCA complex was highly similar to the previously determined apo FoxA (r.m.s.d 0.53 Å) and FoxA-DFOB structures (r.m.s.d. 0.38 Å) (Supplementary Figure 4). NOCA occupies an internal cavity exposed to the extracellular space, forming three hydrogen bonds to the side chains facing the binding site (mainly H374, Y218, Y805), with additional stabilizing contacts mediated by the surrounding aromatic side chains. Comparison of the complexes formed by FoxA with NOCA-Fe and DFOB-Fe shows that the mode of siderophore coordination is essentially the same, albeit with fewer H-bonds between FoxA and NOCA-Fe than with DFOB-Fe (Supplementary Figure 5). The position of the ferri-NOCA and ferri-DFOB siderophores are almost perfectly superimposed based on the position of the Fe atoms (Figure 7A).

We investigated the affinity of iron-loaded NOCA for purified FoxA by tryptophan fluorescence quenching.[26] Titration of ferri-NOCA into purified FoxA led to concentration-dependent quenching of Trp fluorescence and showed the dissociation constant (K_d) to be 178 ± 16 nM, with a 1:1 stoichiometry (Figure 7B), slightly higher than the previously reported K_d of 100 ± 10 nM of ferri-DFOB for FoxA.[26]

It is surprising how perfectly the position of the ferri-NOCA and ferri-DFOB siderophores in FoxA binding site superimpose, with the Fe atoms located at exactly the same position in both complexes. The structure of FoxA was previously crystallized in the apo-form and complexed with DFOB and the periplasmic domain of TonB.[26] These structures and biophysical interaction studies showed that ferri-DFOB binds to the transporter in a two-step TonB-binding mechanism, which must also be true for ferri-NOCA binding.[26] As both ferri-NOCA and ferri-

DFOB complexes share a very similar mode of binding to FoxA, it is not surprising that they activate the signaling pathway involving FoxR/FoxI with similar efficiency for the transcription and expression of FoxA.

Conclusion. In conclusion, we demonstrate that at least two TBDTs, FoxA and FiuA, are involved in iron acquisition by tris-hydroxamate siderophores in *P. aeruginosa* cells. FiuA imports ferri-FRC complexes across the outer membrane and FoxA, ferri-NOCA, and ferri-DFOB complexes. The crystal structure of FoxA shows a very similar binding mode for ferri-NOCA and ferri-DFOB to a common binding site and fluorescence titration experiments gave binding affinities of the same order of magnitude. These data offer new insights into the complexity and specificity of the mechanisms involved in iron acquisition by tris-hydroxamate exosiderophores. They also show how *P. aeruginosa* adapts the expression of its various TBDTS in the presence of such exosiderophores. Siderophore-dependent iron uptake pathways are more and more considered as promising gates for the uptake of antibiotics in a Trojan horse strategy. The ability of *P. aeruginosa* cells to sense the presence of NOCA and the resulting highly efficient iron uptake by NOCA are potential assets for the use of NOCA analogues in antibiotic vectorization strategies.

METHODS

Chemicals. Desferrioxamine B (DFOB), ferrichrome (FRC), and the protonophore carbonyl cyanide *m*-chlorophenylhydrazone (CCCP) were purchased from Sigma-Aldrich and $^{55}FeCl_3$ was purchased from Perkin Elmer. NOCA was purified as previously described.[53]

Bacterial strains and growth conditions. The *P. aeruginosa* PAO1 strains used in this study are listed in Table SM1. When grown in iron restricted medium, bacteria were first grown in LB medium overnight at 30°C. Afterwards, they were washed and resuspended in iron-deficient CAA (casamino acid) medium, containing 5g L^{-1} low-iron CAA (Difco), 1.46 g L^{-1} K_2HPO_4 $3H_2O$, and 0.25 g L^{-1} $MgSO_4$ $7H_2O$, and grown overnight at 30°C. To monitor growth in the presence of siderophores, cells were resuspended again in fresh CAA medium at an optical density of $OD_{600\ nm}$ = 0.1 with or without 10 μM DFOB, NOCA, or FRC in 96 well plates. Plates were incubated at 30°C, with shaking every 15 min, in a microplate reader (Infinite M200, Tecan). Growth was followed by measuring the optical density ($OD_{600\ nm}$) every 30 min, for 20 h.

Construction of fiuA and foxA mutants. Enzymes were obtained from ThermoFisher Scientific. *Escherichia coli* TOP10 (Invitrogen) was used as the host strain for the plasmids. Plasmid construction and primers were as described previously.[9] Briefly, 1,400-bp inserts made up of the flanking sequences of either *foxA* or *fiuA* were cloned into a pEXG2 plasmid using a blunt-end ligation strategy. Plasmids were sequenced before being used to generate chromosomal mutations in a *P. aeruginosa* PAO1 Δ*pvdF*Δ*pchA* strain (Supplementary Table 2) as previously described. Recombinant clones were isolated before being verified by PCR and Sanger sequencing.[9]

RNA extraction. Bacteria were first grown in LB medium overnight at 30°C. Afterwards, they were washed and resuspended in CAA medium and grown over night. After growth, cells were washed, and resuspended at an $OD_{600\ nm}$ of 0.1 in fresh CAA medium with or without one of the tested siderophores (10 μM). Cells were cultivated at 30°C for 8 h. Afterwards, 2.5 x 10^8 cells were mixed with two volumes of RNAprotect Bacteria Reagent (Qiagen). Samples were lysed in Tris-EDTA pH 8.0 containing 15 mg/ml lysozyme (Sigma-Aldrich) for 15 min at 25°C. Then, lysates were homogenized using a QIAshredder kit (Quiagen) and total RNA extracted using an RNeasy mini kit (Quiagen). After treatment with DNase (RNase-Free DNase Set, Qiagen), RNA was purified with an RNeasy Mini Elute cleanup kit (Qiagen).

RT-qPCR analysis. RNA (1μg) was reversed-transcribed using a High Capacity RNA to cDNA kit, in accordance with the manufacturer's instructions (Applied Biosystems). Gene expression was measured in a SpetOne Plus Instrument (Applied Biosystems) using Power Sybr Green PCR Master Mix (Applied Biosystems) and the appropriate primers (listed in Supplementary Table 3). The expression of *uvrD* was used as an internal control. The transcript levels were normalized with respect to those for *uvrD* and expressed as base two logarithms of the ratio (fold-change) relative to the reference conditions.

Iron uptake. Bacteria were grown as for RNA extraction. Complexes of siderophore-^{55}Fe were prepared as previously described[32] in 50 mM Tris-HCl pH 8.0 buffer with a siderophore:iron ratio of 20:1 and as described previously.[9]

Proteomic analysis. Bacteria were grown as for RNA extraction. The cells (5 x 10^8) were harvested and used for proteomic analysis. Each sample was prepared in biological triplicate for each cell-culture condition and the data analyzed as described previously.[9] The MS data

were deposited in the ProteomeXchange Consortium database via the PRIDE[54] partner repository with the dataset identifier PXD020868 (Project DOI: 10.6019/PXD020868). Reviewer account details: **Username:** reviewer99826@ebi.ac.uk **Password:** KTZIlS5w.

Protein expression and purification. Recombinant FoxA was expressed and purified as previously described.[26]

Crystallization and structure determination. For crystallization, FoxA was mixed with a 3- to 4-fold excess NOCA-Fe dissolved in 100% DMSO and set on ice for approximately 30 min. Crystals of FoxA-NOCA-Fe complex were grown in 1.8 M ammonium sulfate, 0.1 M sodium cocadylate pH 6.5, 0.05 M NaCl, cryo-protected by the step-wise addition of glycerol to a final concentration of 18-20% (v/v), and immediately harvested.

X-ray diffraction data were collected at the P14 beamline EMBL, Hamburg. All data were processed with XDS[55] and reduced using AIMLESS.[56,57] Due to diffraction anisotropy, the StarANISO server[58] was used to perform anisotropy correction of the data. Crystals belonged to the $P3_221$ space group, as in the previously determined FoxA-DFOB-Fe structure.[26] The structure was solved using molecular replacement in Phaser [59] using apo FoxA (pdb: 6I96) as the search model and refined to 2.95 Å using REFMAC5.[60,61] The refinement strategy involved TLS and jelly-body settings. All data collection and refinement statistics are summarized in Table 1. Coordinates have been deposited in the Protein Data Bank (pdb: 6Z8A). Figures were prepared using Pymol and UCSF Chimera.

Tryptophan fluorescence quenching experiments. The dissociation constant of NOCA-Fe from FoxA was determined by tryptophan fluorescence quenching using exactly the same protocol as that previously described.[26]

ACKNOWLEDGMENTS

We are grateful to the staff at the P14 beamline (EMBL, Hamburg) and acknowledge access to the Sample Preparation and Characterization (SPC) Facility of the EMBL. This work was partially funded by the *Centre National de la Recherche Scientifique* and grants from the associations Vaincre la Mucoviscidose and Gregory Lemarchal (French associations against cystic fibrosis) and the *Agence Nationale pour la Recherche* (VECTRIUM project, ANR 19-CE18-0011-02). V Normant held a fellowship from the Fondation pour la Recherche Médicale and Q Perraud from the associations Vaincre la Mucoviscidose and Gregory Lemarchal. The mass spectrometry instrumentation at the IBMC was funded by the University of Strasbourg, IdEx "Equipement mi-lourd" 2015. The equipment at the IPHC was partially funded by the French Proteomics Infrastructure (ProFI; ANR-10-INSB-08-03).

Supporting Information Available: This material is available free of charge *via* the Internet.

REFERENCE

(1) Andreini, C.; Bertini, I.; Cavallaro, G.; Holliday, G. L.; Thornton, J. M. Metal ions in biological catalysis: from enzyme databases to general principles. *J Biol Inorg Chem* **2008**, *13* (8), 1205–1218.

(2) Hider, R. C.; Kong, X. Chemistry and biology of siderophores. *Natural product reports* **2011**, *27* (5), 637–657. https://doi.org/10.1039/b906679a.

(3) Loomis, L.; Raymond, K. N. Solution equilibria of enterobactin complexes. *Inorg. Chem.* **1991**, *30*, 906–911.

(4) Albrecht-Gary, A. M.; Crumbliss, A. L. Coordination chemistry of siderophores: thermodynamics and kinetics of iron chelation and release. *Metal Ions Biological Systems* **1998**, *35*, 239–327.

(5) Schalk, I. J.; Mislin, G. L. A.; Brillet, K. Structure, function and binding selectivity and stereoselectivity of siderophore-iron outer membrane transporters. *Curr Top Membr* **2012**, *69*, 37–66. https://doi.org/10.1016/B978-0-12-394390-3.00002-1.

(6) Krewulak, K. D.; Vogel, H. J. TonB or not TonB: Is that the question? *Biochemistry and cell biology* **2011**, *89* (2), 87–97. https://doi.org/10.1139/o10-141.

(7) Celia, H.; Noinaj, N.; Buchanan, S. K. Structure and stoichiometry of the Ton molecular motor. *Int J Mol Sci* **2020**, *21* (2). https://doi.org/10.3390/ijms21020375.

(8) Barber, M. F.; Elde, N. C. Buried treasure: evolutionary perspectives on microbial iron piracy. *Trends Genet.* **2015**, *31* (11), 627–636. https://doi.org/10.1016/j.tig.2015.09.001.

(9) Perraud, Q.; Cantero, P.; Roche, B.; Gasser, V.; Normant, V. P.; Kuhn, L.; Hammann, P.; Mislin, G. L. A.; Ehret-Sabatier, L.; Schalk, I. J. Phenotypic adaption of *Pseudomonas aeruginosa* by hacking siderophores produced by other microorganisms. *Mol. Cell Proteomics* **2020,** *19*(*4*), 589-607. https://doi.org/10.1074/mcp.RA119.001829.

(10) Schalk, I. J.; Rigouin, C.; Godet, J. An overview of siderophore biosynthesis among fluorescent Pseudomonads and new insights into their complex cellular organization. *Environ. Microbiol.* **2020**, *22* (4), 1447–1466. https://doi.org/10.1111/1462-2920.14937.

(11) Ghysels, B.; Dieu, B. T.; Beatson, S. A.; Pirnay, J. P.; Ochsner, U. A.; Vasil, M. L.; Cornelis, P. FpvB, an alternative type I ferripyoverdine receptor of *Pseudomonas aeruginosa*. *Microbiology* **2004**, *150* (Pt 6), 1671–1680.

(12) Brillet, K.; Journet, L.; Celia, H.; Paulus, L.; Stahl, A.; Pattus, F.; Cobessi, D. A β-strand lock-exchange for signal transduction in TonB-dependent transducers on the basis of a common structural motif. *Structure* **2007**, *15*, 1383–1391.

(13) Cobessi, D.; Celia, H.; Pattus, F. Crystallization and X-ray diffraction analyses of the outer membrane pyochelin receptor FptA from *Pseudomonas aeruginosa*. *Acta Crystallogr D Biol Crystallogr* **2004**, *60* (Pt 10), 1919–1921.

(14) Cornelis, P.; Bodilis, J. A survey of TonB-dependent receptors in fluorescent Pseudomonads. *Environmental microbiology reports* **2009**, *1* (4), 256–262. https://doi.org/10.1111/j.1758-2229.2009.00041.x.

(15) Smith, A. D.; Wilks, A. Differential contributions of the outer membrane receptors PhuR and HasR to Heme acquisition in *Pseudomonas aeruginosa*. *J. Biol. Chem.* **2015**, *290* (12), 7756–7766. https://doi.org/10.1074/jbc.M114.633495.

(16) Atanaskovic, I.; Mosbahi, K.; Sharp, C.; Housden, N. G.; Kaminska, R.; Walker, D.; Kleanthous, C. Targeted killing of *Pseudomonas aeruginosa* by pyocin G occurs via the hemin transporter Hur. *Journal of Molecular Biology* **2020**, *432* (13), 3869–3880. https://doi.org/10.1016/j.jmb.2020.04.020.

(17) Poole, K.; Young, L.; Neshat, S. Enterobactin-mediated iron transport in *Pseudomonas aeruginosa*. *J Bacteriol* **1990**, *172* (12), 6991–6996.

(18) Ghysels, B.; Ochsner, U.; Mollman, U.; Heinisch, L.; Vasil, M.; Cornelis, P.; Matthijs, S. The *Pseudomonas aeruginosa* PirA gene encodes a second receptor for ferrienterobactin and synthetic catecholate analogues. *FEMS microbiology letters* **2005**, *246* (2), 167–174.

(19) Moynié, L.; Luscher, A.; Rolo, D.; Pletzer, D.; Tortajada, A.; Weingart, H.; Braun, Y.; Page, M. G. P.; Naismith, J. H.; Köhler, T. Structure and function of the PiuA and PirA siderophore-drug receptors from *Pseudomonas aeruginosa* and *Acinetobacter baumannii*. *Antimicrob. Agents Chemother.* **2017**, *61* (4). https://doi.org/10.1128/AAC.02531-16.

(20) Moynie, L.; Milenkovic, S.; Malloci, G.; Mislin, G. L. A.; Baco, E.; Gasser, V.; Schalk, I. J.; Ceccarelli, M.; Naismith, J. H. The complex of ferric-enterobactin with its transporter suggests a multi-step conformationally coupled process of uptake. *submitted to Nature Com*. **2019**, *10*(*1*),3673-3687. https:// doi: 10.1038/s41467-019-11508-y.

(21) Elias, S.; Degtyar, E.; Banin, E. FvbA Is required for vibriobactin utilization in *Pseudomonas aeruginosa*. *Microbiology* **2011**, *157* (Pt 7), 2172–2180. https://doi.org/10.1099/mic.0.044768-0.

(22) Llamas, M. A.; Mooij, M. J.; Sparrius, M.; Vandenbroucke-Grauls, C. M.; Ratledge, C.; Bitter, W. Characterization of five novel *Pseudomonas aeruginosa* cell-surface signalling systems. *Molecular microbiology* **2008**, *67* (2), 458–472.

(23) Cuiv, P. O.; Clarke, P.; O'Connell, M. Identification and characterization of an iron-regulated gene, ChtA, required for the utilization of the xenosiderophores aerobactin, rhizobactin 1021 and schizokinen by *Pseudomonas aeruginosa. Microbiology* **2006**, *152* (Pt 4), 945–954. https://doi.org/10.1099/mic.0.28552-0.

(24) Marshall, B.; Stintzi, A.; Gilmour, C.; Meyer, J.-M.; Poole, K. Citrate-mediated iron uptake in *Pseudomonas aeruginosa*: involvement of the citrate-inducible FecA receptor

and the FeoB ferrous iron Transporter. *Microbiology (Reading, Engl.)* **2009**, *155* (Pt 1), 305–315. https://doi.org/10.1099/mic.0.023531-0.

(25) Llamas, M. A.; Sparrius, M.; Kloet, R.; Jimenez, C. R.; Vandenbroucke-Grauls, C.; Bitter, W. The heterologous siderophores ferrioxamine B and ferrichrome activate signaling pathways in *Pseudomonas aeruginosa*. *Journal of bacteriology* **2006**, *188* (5), 1882–1891.

(26) Josts, I.; Veith, K.; Tidow, H. Ternary structure of the outer membrane transporter FoxA with resolved signalling domain provides insights into TonB-mediated siderophore uptake. *eLife* **2019**, *8*, e48528. https://doi.org/10.7554/eLife.48528.

(27) Müller, G.; Matzanke, B. F.; Raymond, K. N. Iron transport in *Streptomyces pilosus* mediated by ferrichrome siderophores, rhodotorulic acid, and enantio-rhodotorulic acid. *J. Bacteriol.* **1984**, *160* (1), 313–318.

(28) Drechsel, H.; Winkelmann, G. In *Transition Metals in Microbial Metabolism*; Harwood Academic Publishers: Amsterdam, 1997; pp 1–49.

(29) Dean, C. R.; Poole, K. Expression of the ferric enterobactin receptor (PfeA) of *Pseudomonas aeruginosa*: involvement of a two-component regulatory system. *Mol Microbiol* **1993**, *8* (6), 1095–1103.

(30) Michel, L.; Gonzalez, N.; Jagdeep, S.; Nguyen-Ngoc, T.; Reimmann, C. PchR-box recognition by the AraC-type regulator PchR of *Pseudomonas aeruginosa* requires the siderophore pyochelin as an effector. *Molecular microbiology* **2005**, *58* (2), 495–509.

(31) Llamas, M. A.; Imperi, F.; Visca, P.; Lamont, I. L. Cell-surface signaling in Pseudomonas: stress responses, iron transport, and pathogenicity. *FEMS microbiology reviews* **2014**, *38* (4), 569–597. https://doi.org/10.1111/1574-6976.12078.

(32) Gasser, V.; Baco, E.; Cunrath, O.; August, P. S.; Perraud, Q.; Zill, N.; Schleberger, C.; Schmidt, A.; Paulen, A.; Bumann, D.; Mislin, G. L. A.; Schalk, I. J. Catechol

siderophores repress the pyochelin pathway and activate the enterobactin pathway in *Pseudomonas aeruginosa*: an opportunity for siderophore-antibiotic conjugates development. *Environ. Microbiol.* **2016**, *18* (3), 819–832. https://doi.org/10.1111/1462-2920.13199.

(33) Anderegg, G.; L'Eplattenier, F.; Schwarzenbach, G. Hydroxamatkomplexe III. Eisen(III)-Austausch Zwischen Sideraminen Und Komplexonen. Diskussion der Bildungskonstanten der Hydroxamatkomplexe. *Helvetica Chimica Acta* **1963**, *46* (4), 1409–1422. https://doi.org/10.1002/hlca.19630460436.

(34) Zähner, H.; Bachmann, E.; Hütter, R.; Nüesch, J. Sideramine, Eisenhaltige Wachstumsfaktoren aus Mikroorganismen. *PAT* **1962**, *25* (5), 708–736. https://doi.org/10.1159/000161327.

(35) Yamanaka, K.; Oikawa, H.; Ogawa, H.; Hosono, K.; Shinmachi, F.; Takano, H.; Sakuda, S.; Beppu, T.; Ueda, K. Desferrioxamine E produced by *Streptomyces griseus* stimulates growth and development of *Streptomyces tanashiensis*. *Microbiology,* **2005**, *151* (9), 2899–2905. https://doi.org/10.1099/mic.0.28139-0.

(36) Essén, S. A.; Johnsson, A.; Bylund, D.; Pedersen, K.; Lundström, U. S. Siderophore production by *Pseudomonas stutzeri* under aerobic and anaerobic conditions. *Appl. Environ. Microbiol.* **2007**, *73* (18), 5857–5864. https://doi.org/10.1128/AEM.00072-07.

(37) Berner, I.; Winkelmann, G. Ferrioxamine transport mutants and the identification of the ferrioxamine receptor protein (FoxA) in *Erwinia herbicola* (*Enterobacter agglomerans*). *Biol Met* **1990**, *2* (4), 197–202. https://doi.org/10.1007/BF01141359.

(38) Beare, P. A.; For, R. J.; Martin, L. W.; Lamont, I. L. Siderophore-mediated cell signalling in *Pseudomonas aeruginosa*: divergent pathways regulate virulence factor production and siderophore receptor synthesis. *Mol. Microbiol.* **2003**, *47* (1), 195–207. https://doi.org/10.1046/j.1365-2958.2003.03288.x.

(39) Draper, R. C.; Martin, L. W.; Beare, P. A.; Lamont, I. L. Differential proteolysis of sigma regulators controls cell-surface signalling in *Pseudomonas aeruginosa*: Ppoteolysis in cell-surface signalling pathways. *Molecular Microbiology* **2011**, *82* (6), 1444–1453. https://doi.org/10.1111/j.1365-2958.2011.07901.x.

(40) Lamont, I. L.; Beare, P. A.; Ochsner, U.; Vasil, A. I.; Vasil, M. L. Siderophore-mediated signaling regulates virulence factor production in *Pseudomonas aeruginosa*. *Proceedings of the National Academy of Sciences* **2002**, *99* (10), 7072–7077. https://doi.org/10.1073/pnas.092016999.

(41) Spencer, M. R.; Beare, P. A.; Lamont, I. L. Role of cell surface signaling in proteolysis of an alternative sigma factor in *Pseudomonas aeruginosa*. *J. Bacteriol.* **2008**, *190* (14), 4865–4869. https://doi.org/10.1128/JB.01998-07.

(42) Shirley, M.; Lamont, I. L. Role of TonB1 in pyoverdine-mediated Ssignaling in *Pseudomonas aeruginosa*. *J. Bacteriol.* **2009**, *191* (18), 5634–5640. https://doi.org/10.1128/JB.00742-09.

(43) Draper, R. C.; Martin, L. W.; Beare, P. A.; Lamont, I. L. Differential proteolysis of sigma regulators controls cell-surface signalling in *Pseudomonas aeruginosa*. *Mol. Microbiol.* **2011**, *82* (6), 1444–1453. https://doi.org/10.1111/j.1365-2958.2011.07901.x.

(44) Edgar, R. J.; Xu, X.; Shirley, M.; Konings, A. F.; Martin, L. W.; Ackerley, D. F.; Lamont, I. L. Interactions between an anti-sigma protein and two sigma factors that regulate the pyoverdine signaling pathway in *Pseudomonas aeruginosa*. *BMC Microbiol.* **2014**, *14*, 287. https://doi.org/10.1186/s12866-014-0287-2.

(45) Bishop, T. F.; Martin, L. W.; Lamont, I. L. Activation of a cell surface signaling pathway in *Pseudomonas aeruginosa* requires ClpP protease and new sigma factor synthesis. *Front Microbiol* **2017**, *8*, 2442. https://doi.org/10.3389/fmicb.2017.02442.

(46) Edgar, R. J.; Hampton, G. E.; Garcia, G. P. C.; Maher, M. J.; Perugini, M. A.; Ackerley, D. F.; Lamont, I. L. Integrated activities of two alternative sigma factors coordinate iron acquisition and uptake by *Pseudomonas aeruginosa*. *Mol. Microbiol.* **2017**, *106* (6), 891–904. https://doi.org/10.1111/mmi.13855.

(47) Casas Garcia, G. P.; Perugini, M. A.; Lamont, I. L.; Maher, M. J. The Purification of the ΣFpvI/FpvR20 and ΣPvdS/FpvR20 protein complexes is facilitated at room temperature. *Protein Expr. Purif.* **2019**, *160*, 11–18. https://doi.org/10.1016/j.pep.2019.03.005.

(48) Brandel, J.; Humbert, N.; Elhabiri, M.; Schalk, I. J.; Mislin, G. L. A.; Albrecht-Garry, A.-M. Pyochelin, a siderophore of *Pseudomonas aeruginosa*: physicochemical characterization of the Iron(III), Copper(II) and Zinc(II) complexes. *Dalton Trans* **2012**, *41* (9), 2820–2834.

(49) Albrecht-Gary, A. M.; Blanc, S.; Rochel, N.; Ocacktan, A. Z.; Abdallah, M. A. Bacterial iron transport: coordination properties of pyoverdin PaA, a peptidic siderophore of *Pseudomonas aeruginosa*. *Inorg. Chem.* **1994**, *33*, 6391–6402.

(50) Clément, E.; Mesini, P. J.; Pattus, F.; Abdallah, M. A.; Schalk, I. J. The binding mechanism of pyoverdin with the outer membrane receptor FpvA in *Pseudomonas aeruginosa* is dependent on its iron-loaded status. *Biochemistry* **2004**, *43*, 7954–7965.

(51) Cunrath, O.; Geoffroy, V. A.; Schalk, I. J. Metallome of P*seudomonas aeruginosa*: a role for siderophores. *Environ. Microbiol.* **2016**, *18* (10), 3258–3267. https://doi.org/10.1111/1462-2920.12971.

(52) Winsor, G. L.; Griffiths, E. J.; Lo, R.; Dhillon, B. K.; Shay, J. A.; Brinkman, F. S. L. Enhanced annotations and Ffatures for comparing thousands of Pseudomonas genomes in the Pseudomonas genome database. *Nucleic Acids Res.* **2016**, *44* (D1), D646-653. https://doi.org/10.1093/nar/gkv1227.

(53) Meyer, J. M.; Abdallah, M. A. The fluorescent pigment of *Pseudomonas fluorescens*: biosynthesis, purification and physicochemical Properties. *J Gen Microbiol* **1978**, *107*, 319–328.

(54) Vizcaíno, J. A.; Csordas, A.; del-Toro, N.; Dianes, J. A.; Griss, J.; Lavidas, I.; Mayer, G.; Perez-Riverol, Y.; Reisinger, F.; Ternent, T.; Xu, Q.-W.; Wang, R.; Hermjakob, H. 2016 Update of the PRIDE database and its related tools. *Nucleic Acids Res.* **2016**, *44* (D1), D447-456. https://doi.org/10.1093/nar/gkv1145.

(55) Kabsch, W. XDS. *Acta Crystallogr D Biol Crystallogr* **2010**, *66* (Pt 2), 125–132. https://doi.org/10.1107/S0907444909047337.

(56) Evans, P. Scaling and assessment of data quality. *Acta Crystallogr. D Biol. Crystallogr.* **2006**, *62* (Pt 1), 72–82. https://doi.org/10.1107/S0907444905036693.

(57) Evans, P. R. An introduction to data reduction: space-group determination, scaling and intensity statistics. *Acta Crystallogr. D Biol. Crystallogr.* **2011**, *67* (Pt 4), 282–292. https://doi.org/10.1107/S090744491003982X.

(58) Tickle, I. J.; Flensburg, C.; Keller, P.; Paciorek, W.; Sharff, A.; Vonrheim, C.; Bricogne, G. STARANISO. Cambridge, United Kingdom: Global Phasing Ltd. 2018.

(59) McCoy, A. J.; Grosse-Kunstleve, R. W.; Adams, P. D.; Winn, M. D.; Storoni, L. C.; Read, R. J. Phaser crystallographic software. *J Appl Crystallogr* **2007**, *40* (Pt 4), 658–674. https://doi.org/10.1107/S0021889807021206.

(60) Murshudov, G. N.; Skubák, P.; Lebedev, A. A.; Pannu, N. S.; Steiner, R. A.; Nicholls, R. A.; Winn, M. D.; Long, F.; Vagin, A. A. REFMAC5 for the refinement of macromolecular crystal structures. *Acta Crystallogr. D Biol. Crystallogr.* **2011**, *67* (Pt 4), 355–367. https://doi.org/10.1107/S0907444911001314.

(61) Afonine, P. V.; Grosse-Kunstleve, R. W.; Echols, N.; Headd, J. J.; Moriarty, N. W.; Mustyakimov, M.; Terwilliger, T. C.; Urzhumtsev, A.; Zwart, P. H.; Adams, P. D.

Towards automated crystallographic structure refinement with Phenix.Refine. *Acta Crystallogr. D Biol. Crystallogr.* **2012**, *68* (Pt 4), 352–367. https://doi.org/10.1107/S0907444912001308.

(62) Hannauer, M.; Barda, Y.; Mislin, G. L.; Shanzer, A.; Schalk, I. J. The ferrichrome uptake pathway in *Pseudomonas aeruginosa* involves an iron release mechansim with acylation of the siderophore and a recycling of the modified desferrichrome. *J Bacteriol* **2010**, *192*, 1212–1220. https://doi.org/10.1128/JB.01539-09.

TABLE

Table 1. Data collection and refinement statistics

	FoxA-nocardamine complex (pdb: 6Z8A)
Data collection	
Beamline	PETRA III, P14
Space group	$P3_221$
Cell dimensions	
a, *b*, *c* (Å)	95.2, 95.2, 178.65
α, β, γ (°)	90, 90, 90
Resolution (Å)	82.465-2.95 (3.1-2.95)
R_{merge}	0.18 (2.58)
R_{meas}	0.185 (2.64)
$I / \sigma I$	12.8 (1.4)
$CC_{1/2}$	0.99 (0.697)
Completeness (%)	94 (99)
Redundancy	20 (19.8)
Refinement	
Resolution (Å)	2.95
No. reflections	14984 (750)
R_{work} / R_{free}	0.23/0.27
No. atoms	5396
Protein	5340
Ligand/ion	48
Water	8
B-factors	
Protein	65.3
Ligand/ion	68.2
R.m.s. deviations	
Bond lengths (Å)	0.012
Bond angles (°)	2.056

FIGURE LEGENDS

Figure 1. Chemical structures of siderophores. a) Desferrioxamine E or nocardamine (NOCA), (b) desferrioxamine B (DFOB), and (c) desferrichrome (FRC). Ferric iron is chelated at a 1:1 stoichiometry by these three siderophores. The functional groups involved in iron chelation for each siderophore are shown in red. Affinities of the siderophores for iron are: NOCA, 10^{32} M^{-1}; DFOB, 10^{30} M^{-1}, and FRC, 10^{29} M^{-1}.[33]

Figure 2. Modulation of the expression of proteins involved in iron acquisition in *P. aeruginosa* PAO1 cells grown in CAA medium in the presence of NOCA or DFOB. a) and b) Proteomic analyses were performed on *P. aeruginosa* PAO1 cells grown for 8 h in CAA medium, with or without 10 µM NOCA (a) or DFOB (b). The average values measured in CAA without siderophores were plotted against the average values in CAA supplemented with the siderophores. c) and d) and e) Heat maps of various proteins involved in the PCH (d) and PVD (e) pathways and of TBDTs (c): the darker the shade of green, the higher the expression of the protein is induced; the darker the shade of red, the stronger the expression of protein is repressed. Only the proteins for which a change in the level of expression was observed are shown. Proteins not detected in the three experiments are represented in grey; NS: nonsignificant; *$p < 0.05$, **$p < 0.01$, and ***$p < 0.001$. Sup Data 1 shows the detailed results of protein identification and quantitation. Supplementary Figure 1 shows these proteomic data (volcano plots) considering the log10 of the adjusted p value. The results for FRC were obtained in Perraud *et al.* 2020.[9]

Figure 3. Modulation of the transcription of genes encoding TBDTs involved in iron acquisition in *P. aeruginosa* cells when grown with or without NOCA (a) or DFOB (b). *P. aeruginosa* PAO1 was grown as for the proteomic analyses, with or without 10 µM NOCA (a)

or DFOB (b). Gene transcription was normalized to that of the *uvrD* reference gene. The results show the ratio between the values obtained in the presence of the siderophore over those obtained in the absence of the siderophore. *fptA* encodes the TBDT of PCH, *fpvA* that of PVD, *pfeA* that of enterobactin, *fvbA* that of vibriobactin, *femA* that of mycobactin and carboxymycobactin, *fiuA* that of FRC, *foxA* that of DFO-B, *fecA* that of citrate, and *PA0434* a hypothetical TBDT. The data show the mean of three independent experiments.

Figure 4. ^{55}Fe uptake by *ΔpvdFΔpchA*, *ΔpvdFΔpchAΔfoxA*, *ΔpvdFΔpchAΔfiuA*, and *ΔpvdFΔpchAΔfiuAΔfoxA* cells in the presence of NOCA (a), DFOB (b), or FRC (c). The strains were grown in CAA medium supplemented with one of the siderophores (NOCA, DFOB, or FRC) to induce the expression of the corresponding uptake pathway. Then, bacteria were harvested and incubated in 50 mM Tris-HCl pH 8.0 in the presence of 200 nM of the ^{55}Fe-siderophore complexes. Aliquots were removed at various times, the bacteria pelleted, and the radioactivity retained in the cells measured. In each panel, transport in *ΔpvdFΔpchA* cells is shown in red, that in *ΔpvdFΔpchAΔfoxA* in blue, that in *ΔpvdFΔpchAΔfiuA* in green, and that in *ΔpvdFΔpchAΔfiuAΔfoxA* in black. For each siderophore, the uptake assays with *ΔpvdFΔpchA* cells were also performed in the presence of the protonophore CCCP (orange curve) to differentiate proton-motive force dependent transport from diffusion. For each curve, the data represent the mean of three independent experiments.

Figure 5. Growth of *ΔpvdFΔpchA, ΔpvdFΔpchAΔfoxA*, and *ΔpvdFΔpchAΔfiuA* strains with or without NOCA, DFOB, or FRC. The *ΔpvdFΔpchA* (red curve) and *ΔpvdFΔpchAΔfoxA* (blue curve) strains were grown in CAA medium, with (a) or without 10 μM NOCA (b) or DFOB (c). The *ΔpvdFΔpchA* (red curve) and *ΔpvdFΔpchAΔfiuA* (green curve) strains were grown in CAA medium supplemented (e) or not (d) with 10 μM FRC.

Growth was followed by monitoring optical density at 600 nm. The results are representative of three independent experiments.

Figure 6. Overall structure and siderophore coordination of the FoxA-NOCA complex. a) Cutaway-view of FoxA with Fe^{3+}-NOCA located in the binding pocket. b) Detailed view of the NOCA-binding pocket with interacting residues shown as sticks. c) Polder omit showing electron density for Fe^{3+}-NOCA.

Figure 7. Interactions between FoxA and NOCA-Fe. a) Position of the ferri-NOCA and ferri-DFOB siderophores in the FoxA binding site. Red sphere, ferric iron ion; NOCA in green, and DFOB in blue. b) Fluorescence titration experiments with NOCA fitted using a single-site binding model (left) yield a K_d of 178 ± 16 nM. Raw emission spectra (right) showing the quenching of Trp fluorescence by titration of NOCA.

Figure 8. Proposed model of NOCA, DFOB and FRC dependent iron uptake pathways in *P. aeruginosa*. Ferri-NOCA is transported across the outer membrane exclusively by FoxA TBDT, whereas ferri-DFOB is transported by FoxA and another unidentified TBDT. Both ferri-NOCA and ferri-DFOB induce the transcription and expression of *foxA* via the sigma and anti-sigma (FoxI/FoxR) dependent mechanism. How iron is released from these two siderophores and transported into the bacterial cytoplasm is still unknown. Ferri-FRC is transported across the outer membrane by FiuA and another unidentified TBDT. Once in the periplasm, Ferri-FRC is transported further across the inner membrane by the permease FiuB.[62] Iron is released from FRC by a mechanism involving the acetylation of FRC by FiuE and reduction by an unidentified reductase.[62] Ferri-FRC induces the transcription and expression of *fiuA*[22] and likely that of *fiuB and fiuE* via the sigma and anti-sigma (FiuI/FiuR) dependent mechanism. The inner

membrane complex TonB-ExbBD provides the energy for uptake by the TBDTs in all pathways presented in the figure.[5]

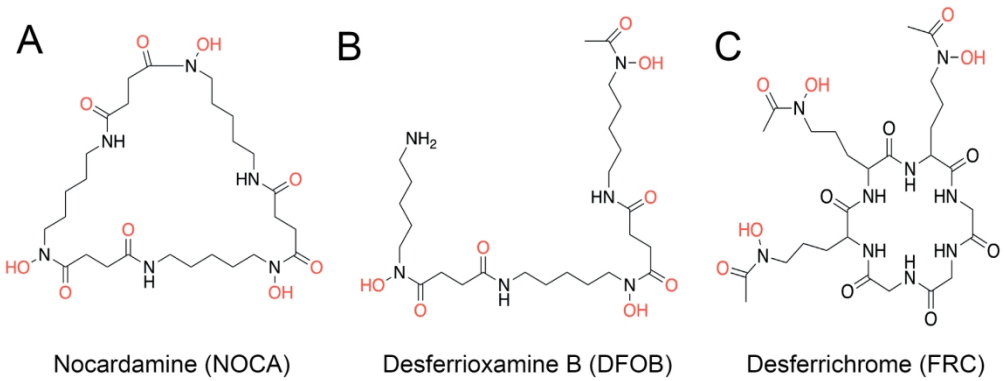

Figure 1. Chemical structures of siderophores. (A) Nocardamine (NOCA) or desferrioxamine E, (B) desferrioxamine B (DFOB), and (C) desferrichrome (FRC). Ferric iron is chelated at a 1:1 stoichiometry by these three siderophores. The functional groups involved in iron chelation for each siderophore are shown in red. Affinities of the siderophores for iron are: NOCA, 10^{32} M^{-1}; DFOB, 10^{30} M^{-1}, and FRC, 10^{29} M^{-1} .[34]

159x60mm (300 x 300 DPI)

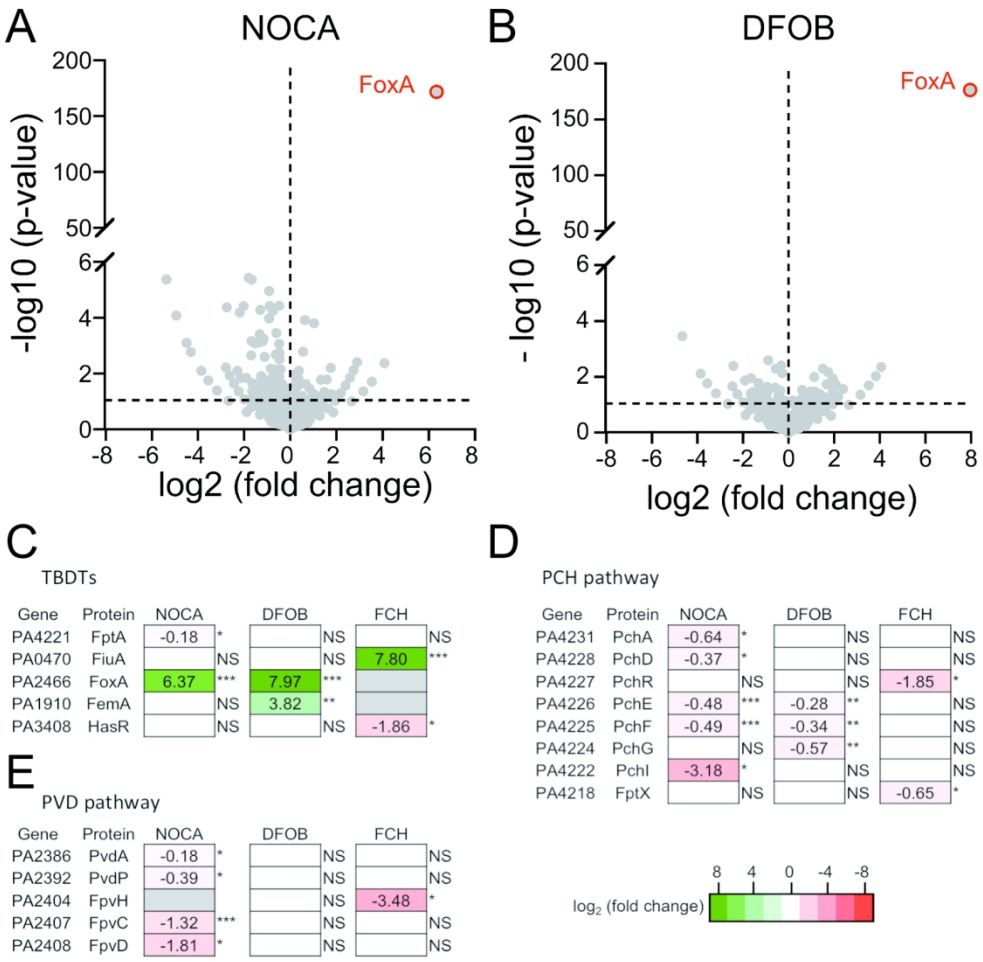

Figure 2. Modulation of the expression of proteins involved in iron acquisition in *P. aeruginosa* PAO1 cells grown in CAA medium in the presence of NOCA or DFOB. A and B. Proteomic analyses were performed on *P. aeruginosa* PAO1 cells grown for 8 h in CAA medium, with or without 10 µM NOCA (A) or DFOB (B). The average values measured in CAA without siderophores were plotted against the average values in CAA supplemented with the siderophores. C, D, and E. Heat maps of various proteins involved in the PCH (D) and PVD (E) pathways and of TBDTs (C): the darker the shade of green, the more expression of the protein is induced. Only the proteins for which a change in the level of expression was observed are shown. Proteins not detected in the three experiments are represented in grey; NS: nonsignificant; *p < 0.05, **p < 0.01, and ***p < 0.001. Sup Data 1 shows the detailed results of protein identification and quantitation. Figure SM1 shows these proteomic data (volcano plots) considering the log10 of the adjusted p value. The results for FCH were obtained in Perraud *et al.* 2020.[10]

159x153mm (300 x 300 DPI)

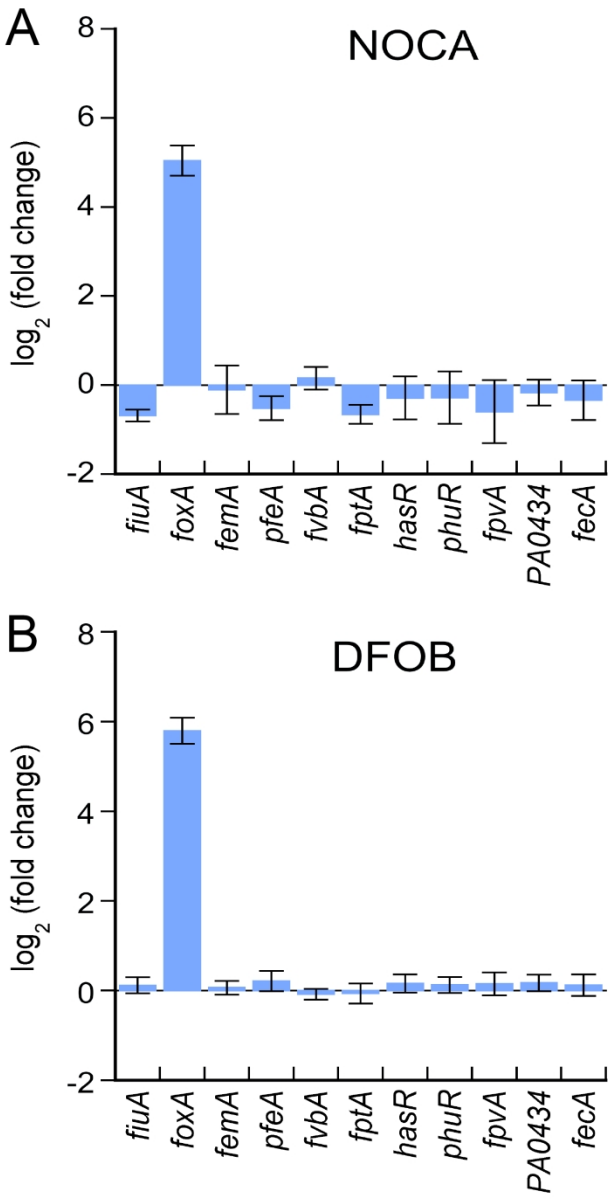

Figure 3. Modulation of the transcription of genes encoding TBDTs involved in iron acquisition in *P. aeruginosa* cells when grown with or without NOCA (A) or DFOB (B). *P. aeruginosa* PAO1 was grown as for the proteomic analyses, with or without 10 µM NOCA (A) or DFOB (B). Gene transcription was normalized to that of the *uvrD* reference gene. The results show the ratio between the values obtained in the presence of the siderophore over those obtained in the absence of the siderophore. *fptA* encodes the TBDT of PCH, *fpvA* that of PVD, *pfeA* that of enterobactin, *fvbA* that of vibriobactin, *femA* that of mycobactin and carboxymycobactin, *fiuA* that of FERRI, *foxA* that of DFO-B, *fecA* that of citrate, and PA0434 a hypothetical TBDT. The data show the mean of three independent experiments.

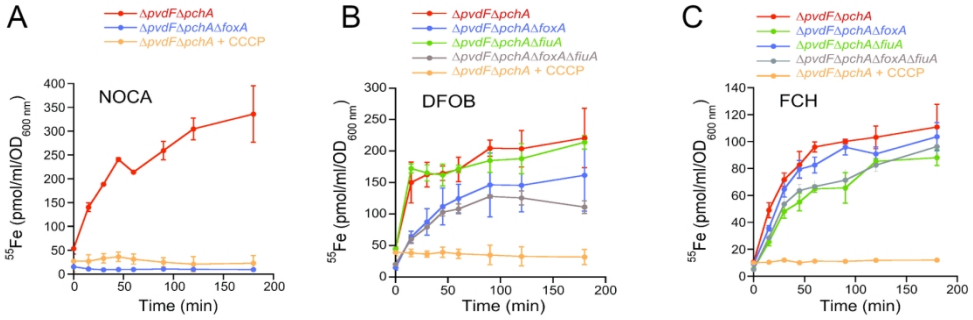

Figure 4. ^{55}Fe uptake by Δ*pvdF*Δ*pchA*, Δ*pvdF*Δ*pchA*Δ*foxA*, Δ*pvdF*Δ*pchA*Δ*fiuA*, and Δ*pvdF*Δ*pchA*Δ*fiuA*Δ*foxA* cells in the presence of NOCA (A), DFOB (B), or FRC (C). The strains were grown in CAA medium supplemented with one of the siderophores (NOCA, DFOB, or FRC) to induce the expression of the corresponding uptake pathway. Then, bacteria were harvested and incubated in 50 mM Tris-HCl pH 8.0 in the presence of 200 nM of the ^{55}Fe-siderophore complexes. Aliquots were removed at various times, the bacteria pelleted, and the radioactivity retained in the cells measured. In each panel, transport in Δ*pvdF*Δ*pchA* cells is shown in red, that in Δ*pvdF*Δ*pchA*Δ*foxA* in blue, that in Δ*pvdF*Δ*pchA*Δ*fiuA* in green, and that in Δ*pvdF*Δ*pchA*Δ*fiuA*Δ*foxA* in black. For each siderophore, the uptake assays with Δ*pvdF*Δ*pchA* cells were also performed in the presence of the protonophore CCCP (orange curve) to differentiate proton-motive force dependent transport from diffusion. For each curve, the data represent the mean of three independent experiments.

160x51mm (300 x 300 DPI)

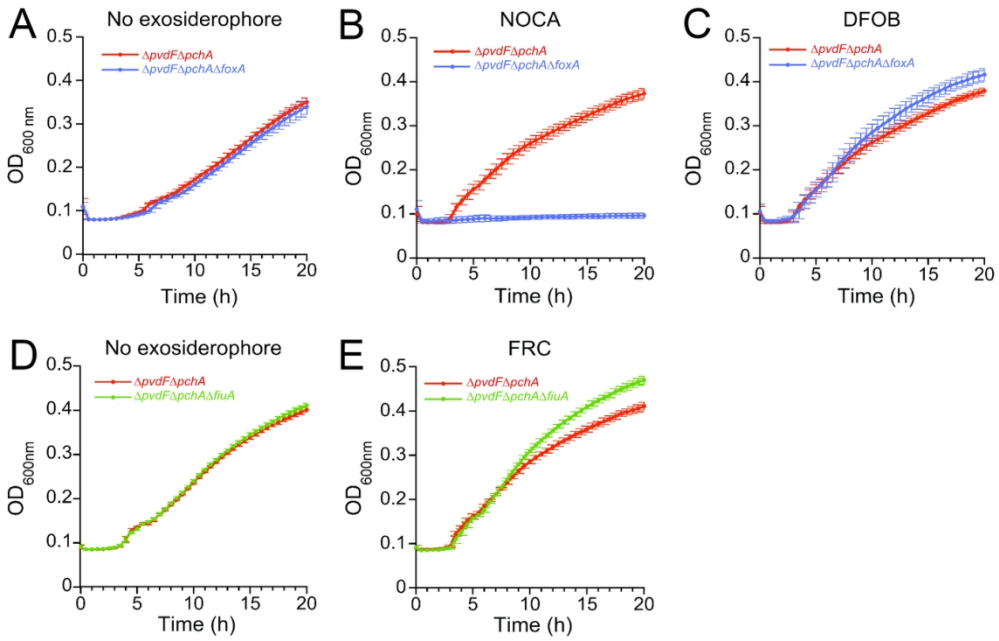

Figure 5. Growth of Δ*pvdF*Δ*pchA*, Δ*pvdF*Δ*pchA*Δ*foxA*, and Δ*pvdF*Δ*pchA*Δ*fiuA* strains with or without NOCA, DFOB, or FRC. The Δ*pvdF*Δ*pchA* (red curve) and Δ*pvdF*Δ*pchA*Δ*foxA* (blue curve) strains were grown in CAA medium, with (A) or without 10 µM NOCA (B) or DFOB (C). The Δ*pvdF*Δ*pchA* (red curve) and Δ*pvdF*Δ*pchA*Δ*fiuA* (green curve) strains were grown in CAA medium supplemented (E) or not (D) with 10 µM FRC. Growth was followed by monitoring optical density at 600 nm. The results are representative of three independent experiments.

119x76mm (300 x 300 DPI)

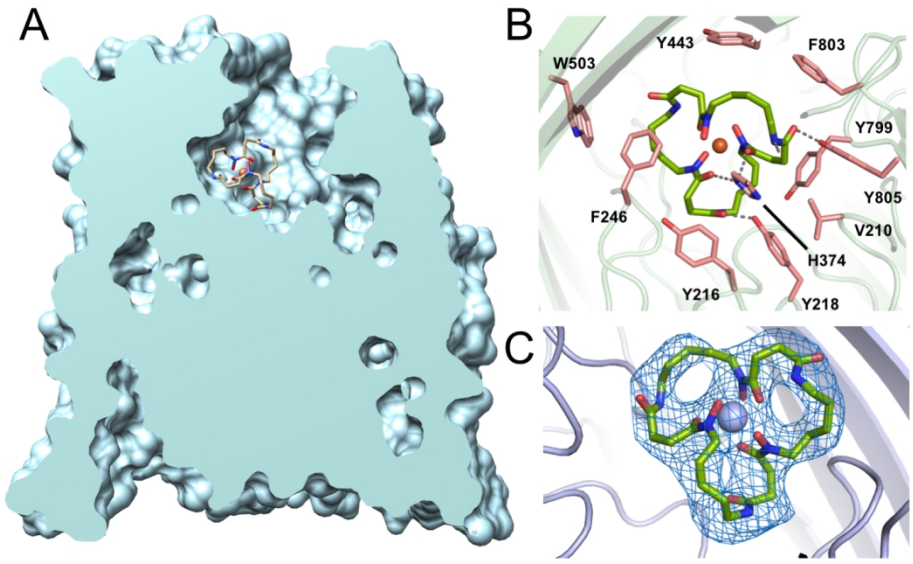

Figure 6. Overall structure and siderophore coordination of the FoxA-NOCA complex. A. Cutaway-view of FoxA with Fe^{3+}-NOCA located in the binding pocket. B. Detailed view of the NOCA-binding pocket with interacting residues shown as sticks. C. Polder omit showing electron density for Fe^{3+}-NOCA.

159x99mm (247 x 247 DPI)

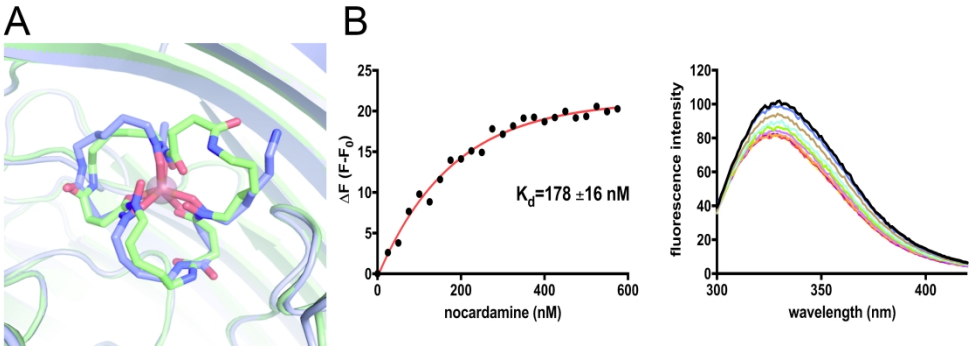

Figure 7. Interactions between FoxA and NOCA-Fe. A. Position of the ferri-NOCA and ferri-DFOB siderophores in the FoxA binding site. Red sphere, ferric iron ion; NOCA in green, and DFOB in blue. B. Fluorescence titration experiments with NOCA fitted using a single-site binding model (left) yield a Kd of 178 ± 16 nM. Raw emission spectra (right) showing the quenching of Trp fluorescence by titration of NOCA.

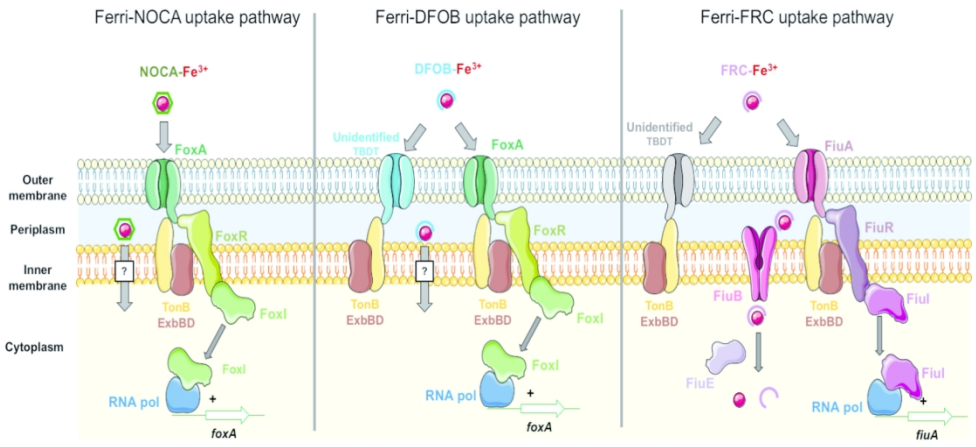

Figure 8. Proposed model of NOCA, DFOB and FRC dependent iron uptake pathways in *P. aeruginosa*. Ferri-NOCA is transported across the outer membrane exclusively by FoxA TBDT, whereas ferri-DFOB is transported by FoxA and another unidentified TBDT. Both ferri-NOCA and ferri-DFOB induce the transcription and expression of *foxA* via the sigma and anti-sigma (FoxI/FoxR) dependent mechanism. How iron is released from these two siderophores and transported into the bacterial cytoplasm is still unknown. Ferri-FRC is transported across the outer membrane by FiuA and another unidentified TBDT. Once in the periplasm, Ferri-FRC is transported further across the inner membrane by the permease FiuB.[43] Iron is released from FRC by a mechanism involving the acetylation of FRC by FiuE and reduction by an unidentified reductase.[43] Ferri-FRC induces the transcription and expression of *fiuA* [23] and likely that of *fiuB* and *fiuE via* the sigma and anti-sigma (FiuI/FiuR) dependent mechanism. The inner membrane complex TonB-ExbBD provides the energy for uptake by the TBDTs in all pathways presented in the figure 6.

160x71mm (300 x 300 DPI)

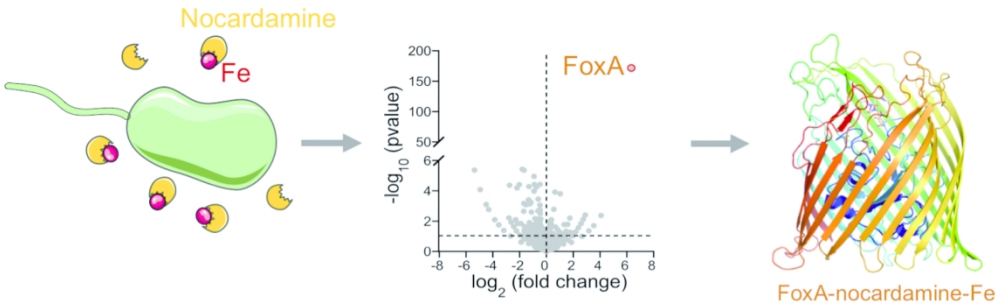

The presence of nocardamine-Fe induces the expression of the transporter FoxA in *P. aeruginosa* cells

159x79mm (300 x 300 DPI)